Hindawi
Advances in Mathematical Physics
Volume 2022, Article ID 9033324, 12 pages
https://doi.org/10.1155/2022/9033324

Research Article

An Analytical and a Numerical Method for Nonlinear Convection-Radiation Problems in Porous Fins

E. D. Correa,[1] J. M. Quirino,[1] R. L. Sobral,[2] J. F. Corrêa,[1] and R. M. S. Gama[1]

[1]*State University of Rio de Janeiro, Rua São Francisco Xavier, 524, Rio de Janeiro, RJ 20550-013, Brazil*
[2]*Federal Center of Technological Education, Est. Adrianopolis, 1317, Nova Iguaçu, RJ 26041-271, Brazil*

Correspondence should be addressed to R. M. S. Gama; rsggama@gmail.com

Received 5 November 2021; Revised 21 December 2021; Accepted 30 December 2021; Published 25 January 2022

Academic Editor: Ming Mei

The present work shows an analytical and a numerical method for heat transfer nonlinear problems in porous fins using the Darcy model. Numerical simulations are carried out with the aid of a sequence of linear problems, each of them possessing an equivalent minimum principle, that has as its limit the solution of the original problem. The nonlinear convection-radiation heat transfer process is considered and simulated by means of a finite difference scheme. Results showed the relevance of the radiation for realistic thermal mapping in porous media with percentage errors of up to 40% for the last nodes.

1. Introduction

In general, the first choice for the enhancement of rate of heat transfer from/to a body consists of using fins in order to provide an increase of the effective heat transfer surface. Since the need of optimizing heat transfer processes is encountered in several practical situations, the study of the thermal behavior of fins becomes a fundamental issue in the heat transfer area.

Nowadays, high-performance heat transfer components are related to the need to achieve high heat transfer rates with low cost and, above all, limited space and weight. Heat transfer on extended surfaces is, currently, one of the main focuses of high-performance heat transfer studies, accounting for the most varied parameters and respective behavior in the thermal mapping [1–3].

The extended surface is widely used in several engineering systems that incorporate from well-known heat exchangers to heat pipes as shown in recent studies [4–6]. Effective sizing of fins and heat sinks requires accurate knowledge of heat transfer on extended surfaces. Usually, convection and conduction heat transfers are the main considered mechanisms, but radiation heat transfer has significant effect in specific applications mainly involving high temperatures and/or rarefied atmospheres [7, 8].

Due the larger effective surface area, porous fins have better thermal performance when compared to conventional solid ones with equivalent size. In the literature, porous constituents of high thermal conductivity have been used to improve the thermal performance of different thermal systems. Bioengineering, electronic technologies, and especially the most recent nanotechnology have been concerned with knowing the effects of heat transfer in porous media.

Some studies leveraged the application the porous fins. Pop et al. [9] conducted analyses of steady-state conjugate free convection about a vertical fin embedded in a porous medium.

Huang and Vafai [10] presented an investigation of forced convection enhancement in a channel using multiple emplaced porous blocks.

Kim et al. [11] experimentally investigated the impact of porous fins on the pressure drop and heat transfer characteristics in plate-fin heat exchangers.

Kiwan [12] introduced a simple method of analysis to study the performance of porous fins in a natural convection environment.

El-Hakiem and Rashad (2007) [13] examined the effects of both radiation and the nonlinear Forchheimer terms on free convection from a vertical cylinder embedded in a fluid-saturated porous medium with the fluid viscosity

varying as an inverse linear function of temperature. Rashad [14] employed magnetohydrodynamics and thermal radiation effects in heat and mass transfer of a vertical flat plate embedded in a fluid saturated porous media.

Kundu and Bhanja [15] developed an analytical model for determination of the performance and optimum dimensions of porous fins accounting for different models of predictions. Gorla and Bakier [16] considered radiation and convection effects in porous media on rectangular profile fin.

Rashad et al. [17] investigated theoretically the effects of thermal radiation and the nonlinear Forchheimer terms on boundary-layer flow and heat transfer by non-Darcy natural convection from a vertical cylinder embedded in a porous medium saturated with nanofluids. Rashad et al. [18] studied the combined effects of thermal radiation and thermophoresis on heat and mass transfer by mixed convection over a vertical rotating cone in a fluid saturated porous medium.

Darvishi et al. [19] conducted a numerical study of steady-state heat transfer in porous rectangular fin under the influence of natural convection and radiation using homotopy analysis method. Darvishi et al. [20] numerically investigated the transient thermal effect on porous fin performance and the comparative study between the fin with or without radiation. Darvishi et al. [21] solved energy equation with spectral collocation method on wet longitudinal fin under natural convection and radiation.

Sobamowo [22] analyzed the heat transfer in porous fin with temperature-dependent thermal conductivity. Results show that increases in convective and porosity parameter improved the efficiency of the fin. Jooma and Harley [23] numerically verified heat transfer in a porous radial fin with the differential transformation method.

Sowmya et al. [24] numerically studied the thermal behavior of a porous longitudinal fin under convection-radiation effect. The nonlinear partial differential equation was nondimensionalized and solved numerically with the help of Maple software by the finite difference method.

This work presents an analytical and numerical method for heat transfer nonlinear problems in porous fins. The Darcy model is utilized to simulate the flow through the porous media. Conduction-radiation-convection heat transfer process is an inherently nonlinear phenomenon in which the coupling on the boundary of the body is mathematically represented by a nonlinear relationship between the absolute temperature and its normal derivative, in which the unknown is the temperature distribution. The solution to the problem is given by the limit of a sequence whose elements are obtained, each one, from the minimization of a quadratic functional.

2. Mathematical Model

The modeling of heat transfer that occurs in a porous radial fin requires several feasibility considerations in its analysis. This study comprises such an analysis considering the material that constitutes the fin as being isotropic and homogeneous, in addition to the fin being analyzed as a strict heat sink. Regarding the fin geometry, this work considers a radial fin, being analyzed in cylindrical coordinates, which is connected to a tubular body, as exemplified in Figure 1.

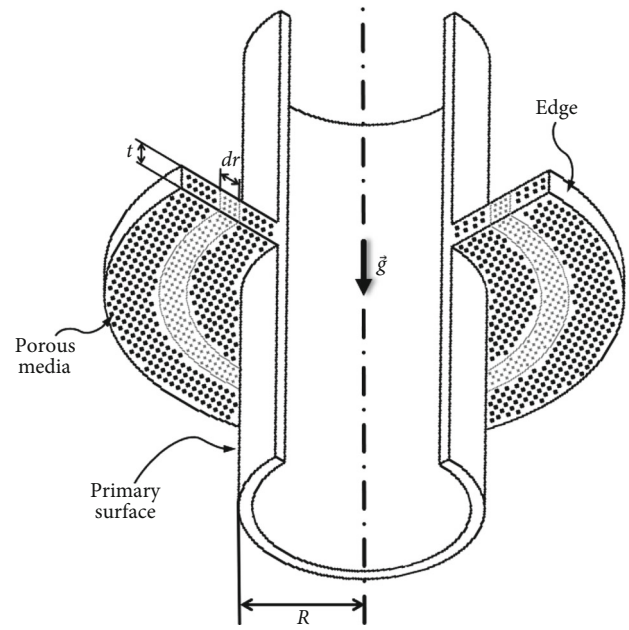

Figure 1: Radial porous fin.

Analyzing the fin as a porous medium leads to infiltration of the fluid in which the fin is inserted, thus allowing a greater exchange of heat between them. The general heat exchange equation used in this work arises from

$$q(x) - q(x + \Delta x) = \dot{m} c_p [T(x) - T_\infty] + hP\Delta x [T(x) - T_\infty] + P\Delta x \sigma \varepsilon \left[T^4(x) - \frac{\alpha_f}{\varepsilon} T_\infty^4 \right], \tag{1}$$

where the fluid mass flow rate is

$$\dot{m} = \rho v_w \Delta x W, \tag{2}$$

in which the interactions between the porous medium and the fluid are described by the Darcy law and Boussinesq approximation, which provides the model

$$v_w(x) = \frac{gK\beta_f}{\nu} [T(x) - T_\infty]. \tag{3}$$

The Fourier law of thermal conduction states that

$$q = -k_{\text{eff}} A_c \frac{dT}{dx}. \tag{4}$$

Combining the equations, evaluating at $\Delta x \longrightarrow 0$, and assuming that $\alpha_f = \varepsilon$, we can rewrite Equation (1), adapting it to cylindrical coordinates, such as

$$\frac{1}{r}\frac{d}{dr}\left(r\frac{dT}{dr}\right)-\frac{\rho_f g\beta_f K}{\nu_f k_{\text{eff}} t}(T-T_a)--\frac{2\varepsilon\sigma F_{f-a}}{k_{\text{eff}} t}\left(|T|^3 T\right)=0. \tag{5}$$

The term $|T|^3 T$ is used to ensure coerciveness, since the function for the temperature T is strictly increasing, in all applied temperature values, ensuring the correct physical description of the phenomenon. [25]

By rearranging the equation so that its algebraic manipulation is convenient, you can rewrite Equation (6) as

$$\frac{d^2T}{dr^2}+\frac{1}{r}\frac{dT}{dr}-A[|T-T_\infty|(T-T_\infty)]-B\left[\left(|T|^3 T\right)-T_\infty^4\right]=0, \tag{6}$$

where the constant A gathers all flow and geometric parameters that affect the solution of the problem and B characterizes the radiation parameter, which carries the effects of the porous body's emissivity.

For a more comprehensive mathematical analysis, it is convenient that the temperature values and the geometric position values will be dimensionless through the following relationships:

$$\theta=\frac{T(r)}{T_b},\qquad \xi=\frac{r}{R}. \tag{7}$$

This equation is considered by being subject to the following boundary conditions:

$$\xi=1\longrightarrow\theta=T_b=1(\text{base}),\qquad \xi=R\longrightarrow\frac{d\theta}{d\xi}=0(\text{tip}). \tag{8}$$

In order to seek possible approaches to the problem, it is assumed that the solution θ of the original problem is given by

$$\theta=\lim_{i\longrightarrow\infty}\left[\varphi^{(i)}\right]. \tag{9}$$

That is, the solution of the problem analyzed by this work is given by the limit of the sequence $[\varphi^{(1)},\varphi^{(2)},\varphi^3,\cdots]$, whose elements are obtained from

$$\frac{1}{\xi}\frac{d}{d\xi}\left(\xi\frac{d\varphi^{(i+1)}}{d\xi}\right)-\alpha\varphi^{(i+1)}+\beta^{(i)}=0,$$
$$\beta^{(i)}=\alpha\varphi^{(i)}-A\left|\varphi^{(i)}-T_\infty\right|\left(\varphi^{(i)}-T_\infty\right)-B\left[\left|\varphi^{(i)}\right|^3\varphi^{(i)}-T_\infty^4\right]. \tag{10}$$

If we consider that $\varphi^{(i)}$ is known, the problem described by Equation (11) is a classical linear boundary value problem, which can be easily solved. Therefore, to ensure that the solution is applicable to the problem, evidence of some aspects of the problem must be presented. The constant α will be discussed in more depth later.

2.1. Nondecreasing Proof. In order to prove that the sequence of $\varphi^{(i)}$ is nondescending, the difference between two consecutive terms of the sequence is considered.

$$\begin{aligned}&\frac{1}{\xi}\frac{d}{d\xi}\left[\xi\frac{d}{d\xi}\left(\varphi^{(i+1)}-\varphi^{(i)}\right)\right]-\alpha\left(\varphi^{(i+1)}-\varphi^{(i)}\right)\\&+\alpha\left(\varphi^{(i)}-\varphi^{(i-1)}\right)-A\left|\varphi^{(i)}-T_\infty\right|\left(\varphi^{(i)}-T_\infty\right)\\&-B\left[\left|\varphi^{(i)}\right|^3\varphi^{(i)}-T_\infty^4\right]++A\left|\varphi^{(i-1)}-T_\infty\right|\left(\varphi^{(i-1)}-T_\infty\right)\\&+B\left[\left(\left|\varphi^{(i-1)}\right|^3\varphi^{(i-1)}\right)-T_\infty^4\right]=0.\end{aligned} \tag{11}$$

Since

$$\varphi\wedge^{(i+1)}(1)-\varphi\wedge^{(i)}(1)=0,\qquad \frac{d}{d\xi}\left(\varphi\wedge^{(i+1)}-\varphi\wedge^{(i)}\right)\Big|_{\xi=R}=0, \tag{12}$$

defining the function $\varphi^{(1)}$as the solution of

$$\begin{aligned}&\frac{1}{\xi}\frac{d}{d\xi}\left[\xi\frac{d}{d\xi}\left(\varphi^{(1)}-\varphi^{(0)}\right)\right]-\alpha\left(\varphi^{(1)}-\varphi^{(0)}\right)\\&=A\left|\varphi^{(0)}-T_\infty\right|\left(\varphi^{(0)}-T_\infty\right)-B\left[\left|\varphi^{(0)}\right|^3\varphi^{(0)}-T_\infty^4\right]\geq 0\end{aligned} \tag{13}$$

with

$$\varphi\wedge^{(1)}(1)=1,\qquad \left(\frac{d\varphi\wedge^{(1)}}{d\xi}\right)\Big|_{\xi=R_{\text{ext}}}=0, \tag{14}$$

we have, since $\varphi^0\equiv 0$, that

$$\varphi^{(1)}-\varphi^{(0)}\geq 0\Rightarrow\varphi^{(1)}\geq\varphi^{(0)}\equiv 0. \tag{15}$$

So, we can write $(i=1)$

$$\begin{aligned}&\frac{1}{\xi}\frac{d}{d\xi}\left[\xi\frac{d}{d\xi}\left(\varphi^{(2)}-\varphi^{(1)}\right)\right]-\alpha\left(\varphi^{(2)}-\varphi^{(1)}\right)+\alpha\left(\varphi^{(1)}-\varphi^{(0)}\right)\\&-A\left|\varphi^{(1)}-T_\infty\right|\left(\varphi^{(1)}-T_\infty\right)-B\left[\left|\varphi^{(1)}\right|^3\varphi^{(1)}-T_\infty^4\right]\\&+A\left|\varphi^{(0)}-T_\infty\right|\left(\varphi^{(0)}-T_\infty\right)+B\left[\left|\varphi^{(0)}\right|^3\varphi^{(0)}-T_\infty^4\right]=0\end{aligned} \tag{16}$$

with

$$\varphi\wedge^{(2)}(1) - \varphi\wedge^{(1)}(1) = 0,$$
$$\frac{d}{d\xi}\left(\varphi\wedge^{(2)} - \varphi\wedge^{(1)}\right)\Big|_{\xi=R_{\text{ext}}} = 0. \tag{17}$$

So, choosing α large enough for ensuring that

$$\alpha\left(\varphi^{(1)} - \varphi^{(0)}\right) \geq A\left|\varphi^{(1)} - T_\infty\right|\left(\varphi^{(1)} - T_\infty\right) + B\left[\left|\varphi^{(1)}\right|^3\varphi^{(1)} - T_\infty^4\right] - A\left|\varphi^{(0)} - T_\infty\right| \cdot \left(\varphi^{(0)} - T_\infty\right) - B\left[\left|\varphi^{(0)}\right|^3\varphi^{(0)} - T_\infty^4\right], \tag{18}$$

the following inequality holds:

$$\varphi^{(2)} \geq \varphi^{(1)} \geq \varphi^{(1)} \equiv 0. \tag{19}$$

Repeating the above procedure, we have

$$\cdots \geq \varphi^{(i+1)} \geq \varphi^{(i)} \geq \varphi^{(i-1)} \geq \cdots \geq \varphi^{(1)} \geq \varphi^{(0)} \equiv 0 \tag{20}$$

provided the constant α is large enough to ensure that

$$\alpha \geq \frac{A\left|\varphi^{(i+1)} - T_\infty\right|\left(\varphi^{(i+1)} - T_\infty\right)}{\varphi^{(i+1)} - \varphi^{(i)}} + \frac{B\left[\left|\varphi^{(i+1)}\right|^3\varphi^{(i+1)} - T_\infty^4\right]}{\varphi^{(i+1)} - \varphi^{(i)}} - \frac{A\left|\varphi^{(i)} - T_\infty\right|\left(\varphi^{(i)} - T_\infty\right) - B\left[\left|\varphi^{(i)}\right|^3\varphi^{(i)} - T_\infty^4\right]}{\varphi^{(i+1)} - \varphi^{(i)}}. \tag{21}$$

It is sufficient to choose α in such a way that

$$\alpha \geq \left[\frac{d}{d\theta}A|\theta - T_\infty|(\theta - T_\infty) + B\left(|\theta|^3\theta - T_\infty^4\right)\right]_{\theta=1} = \left[2A|\theta - T_\infty| + 4B\theta^3\right]_{\theta=1} = 2A|T_\infty| + 4B. \tag{22}$$

2.2. Upper Bound. Combining the above problems, we have

$$\frac{1}{\xi}\frac{d}{d\xi}\left[\xi\frac{d}{d\xi}\left(\theta - \varphi^{(i+1)}\right)\right] + \alpha\left(\varphi^{(i+1)} - \varphi^{(i)}\right) - \left[-A|\theta - T_\infty|(\theta - T_\infty) + B\left[|\theta|^3\theta - T_\infty^4\right] - A\left|\varphi^{(i)} - T_\infty\right| \cdot \left(\varphi^{(i)} - T_\infty\right) - B\left[\left|\varphi^{(i)}\right|^3\varphi^{(i)} - T_\infty^4\right]\right] = 0, \tag{23}$$

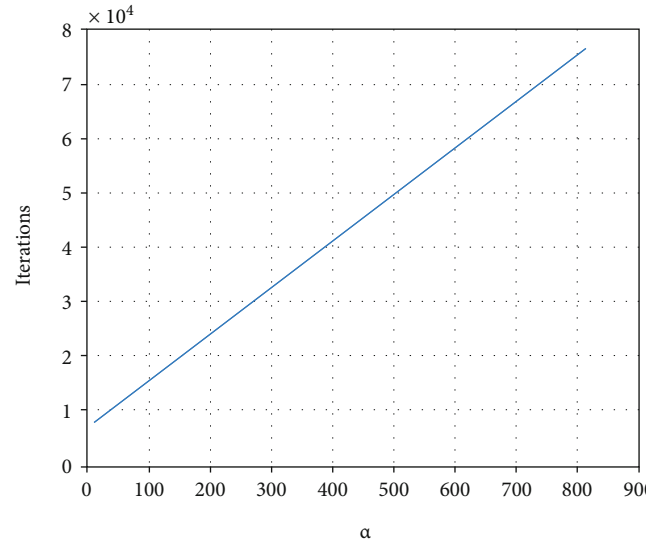

Figure 2: Alpha vs. required iterations.

with the boundary conditions

$$\theta - \varphi^{(i+1)} = 0 \text{at} \xi = 1,$$
$$\frac{d}{d\xi}\left(\theta - \varphi^{(i+1)}\right) = 0 \text{at} \xi = R. \tag{24}$$

Now, let us assume that $(\theta - \varphi^{(i+1)})$ is negative at some point. Since

$$\frac{1}{\xi}\frac{d}{d\xi}\left[\xi\frac{d}{d\xi}\left(\theta - \varphi^{(i+1)}\right)\right] - \alpha\left(\theta - \varphi^{(i+1)}\right) - \left[-A|\theta - T_\infty|(\theta - T_\infty) + B\left[|\theta|^3\theta - T_\infty^4\right] - A\left|\varphi^{(i)} - T_\infty\right|\left(\varphi^{(i)} - T_\infty\right) - B\left[\left|\varphi^{(i)}\right|^3\varphi^{(i)} - \theta_\infty^4\right]\right] = 0, \tag{25}$$

we must have

$$\alpha\left(\theta - \varphi^{(i+1)}\right) - A|\theta - T_\infty|(\theta - T_\infty) + B\left[|\theta\,|\,\theta^3 - T_\infty^4\right] - A\left|\varphi^{(i)} - T_\infty\right|\left(\varphi^{(i)} - T_\infty\right) - B\left[\left|\varphi^{(i)}\right|^3\varphi^{(i)} - \theta_\infty^4\right] \leq 0. \tag{26}$$

Since $\theta \geq 0$, $\varphi^0 \equiv 0$, and α is large enough, we conclude that the above inequality never holds and, so, $(\theta - \varphi^{(1)})$ is nonnegative everywhere. Repeating this procedure, we can conclude that $\theta \geq \varphi^{(i)}$, for any i. In other words, θ is an upper bound for the elements $\varphi^{(i)}$. This ensures the existence of the limit $\theta = \lim_{i\longrightarrow\infty}\varphi^{(i)}$.

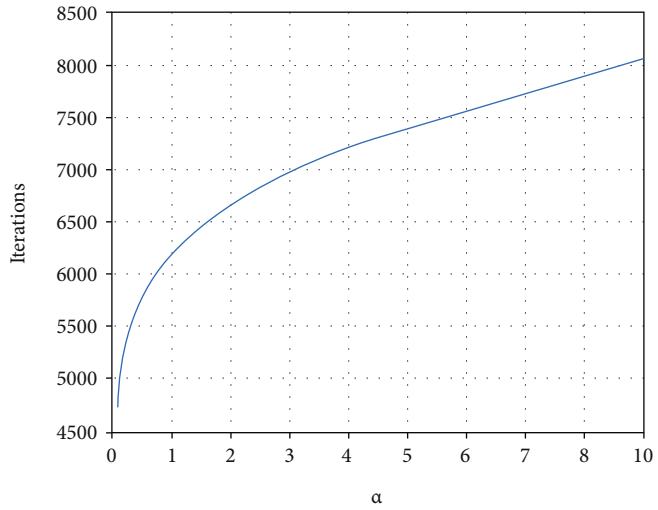

Figure 3: Alpha vs. iterations, for small alpha.

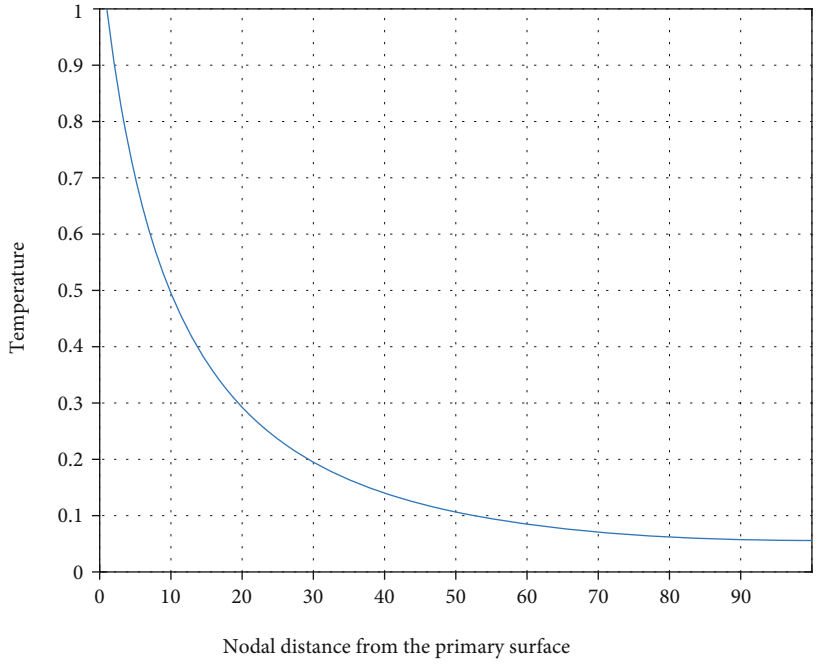

Figure 4: Thermal profile.

2.3. Exact Solution. The maximum of $\theta - \varphi^{(i+1)}$ occurs when its second derivative is not positive. So, this maximum occurs when

$$\alpha\left(\varphi^{(i+1)} - \varphi^{(i)}\right) \geq \left[A|\theta - T_\infty|(\theta - T_\infty) + B\left[|\theta|^3\theta - T_\infty^4\right]\right. - A\left|\varphi^{(i)} - T_\infty\right|\left(\varphi^{(i)} - T_\infty\right) - B\left[\left|\varphi^{(i)}\right|^3\varphi^{(i)} - T_\infty^4\right]\Bigg]. \tag{27}$$

Since the sequence $[\varphi^{(0)}, \varphi^{(1)}, \varphi^{(2)}, \varphi^3]$ has an upper bound and $A|\theta - T_\infty|(\theta - T_\infty) + B[\theta^4 - T_\infty^4]$ is a strictly increasing function, we can conclude that the limit of the sequence is the solution of the original problem.

3. Numerical Analysis

The problem is modeled as

$$\frac{1}{\xi}\frac{d}{d\xi}\left(\xi\frac{d\varphi^{(i+1)}}{d\xi}\right) - \alpha\varphi^{(i+1)} + \beta^{(i)} = 0. \tag{28}$$

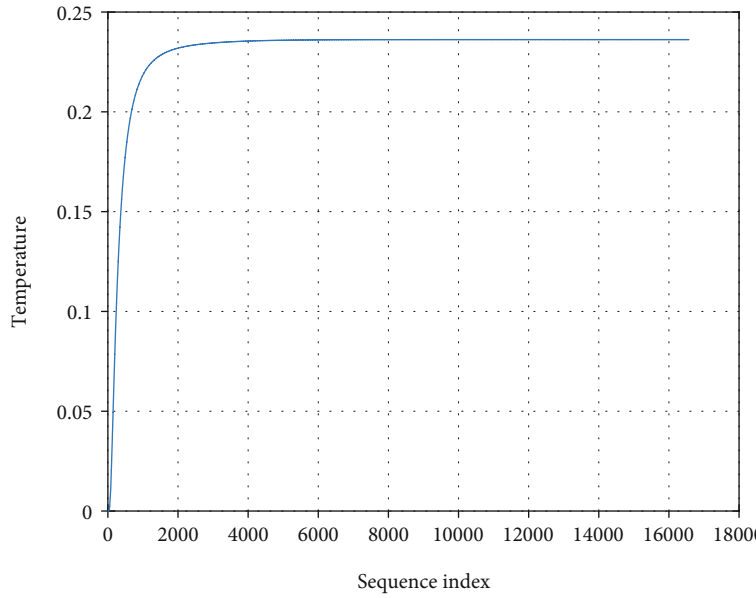

Figure 5: Sequence behavior at point 0.25.

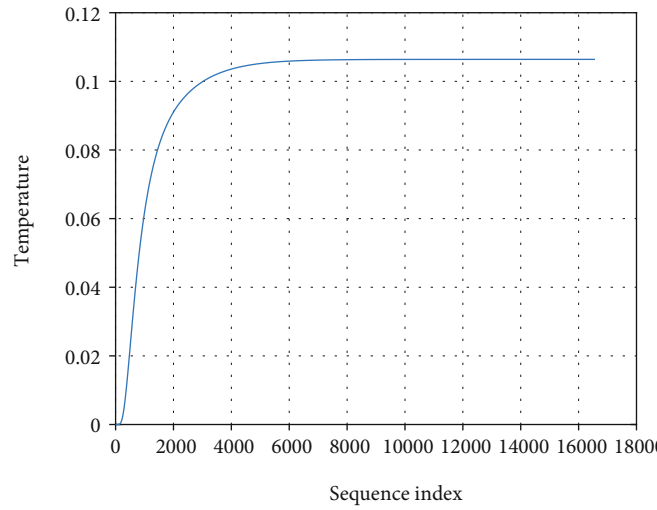

Figure 6: Sequence behavior at point 0.5.

with

$$\beta^{(i)} = \alpha\varphi^{(i)} - A\left|\varphi^{(i)} - T_\infty\right|\left(\varphi^{(i)} - T_\infty\right) - B\left[\left|\varphi^{(i)}\right|^3\varphi^{(i)} - T_\infty^4\right] \tag{29}$$

that has, as its solution the limit of the sequence $[\varphi^0, \varphi^1, \varphi^2, \varphi^3 \cdots]$, where we chose to use the finite difference method to solve the ODE.

Thus, the numerical model adopted becomes

$$\varphi_n^{(i+1)} = \frac{l}{2+\alpha l^2}\left[\frac{\varphi_{n+1}^{(i+1)} + \varphi_{n-1}^{(i+1)}}{l} + \frac{\varphi_{n+1}^{(i+1)} - \varphi_{n-1}^{(i+1)}}{2\xi_n} + \beta_n^{(i)} l\right], \tag{30}$$

where

$$\beta_n^{(i)} = \alpha\varphi_n^{(i)} - \left[A \mid \varphi_n^{(i)} - T_\infty \mid \left(\varphi_n^{(i)} - T_\infty\right)\right] - \left[B\left(\left|\varphi_n^{(i)}\right|^3\left(\varphi_n^{(i)}\right) - T_\infty^4\right)\right]. \tag{31}$$

Therefore, it can be understood that i is the index that represents the numerical iteration comprising each element of the sequence whose limit is the solution to the problem.

Meanwhile, n is the index that represents the numerical iterations of each point in space (geometric) along the radial fin.

A more in-depth study of α demonstrates that the larger its value, the larger the number of iterations required to ensure sequence convergence, as can be seen in Figure 2.

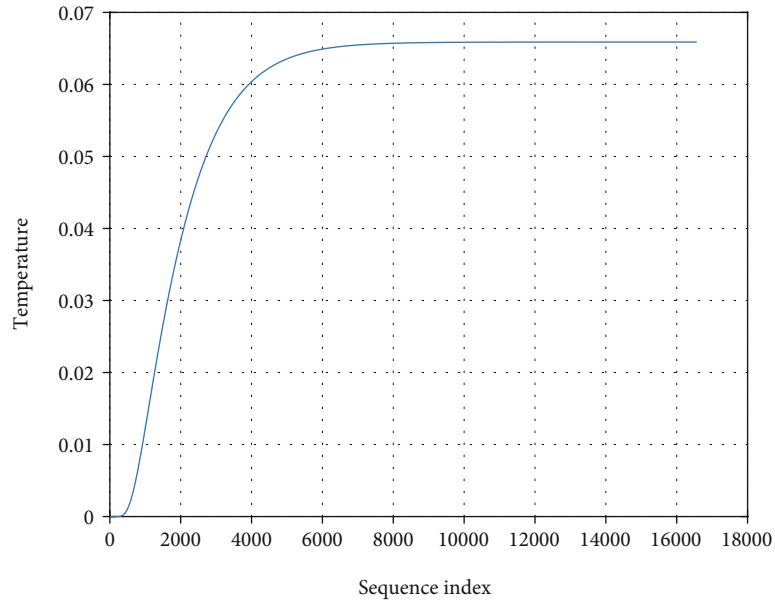

Figure 7: Sequence behavior at point 0.75.

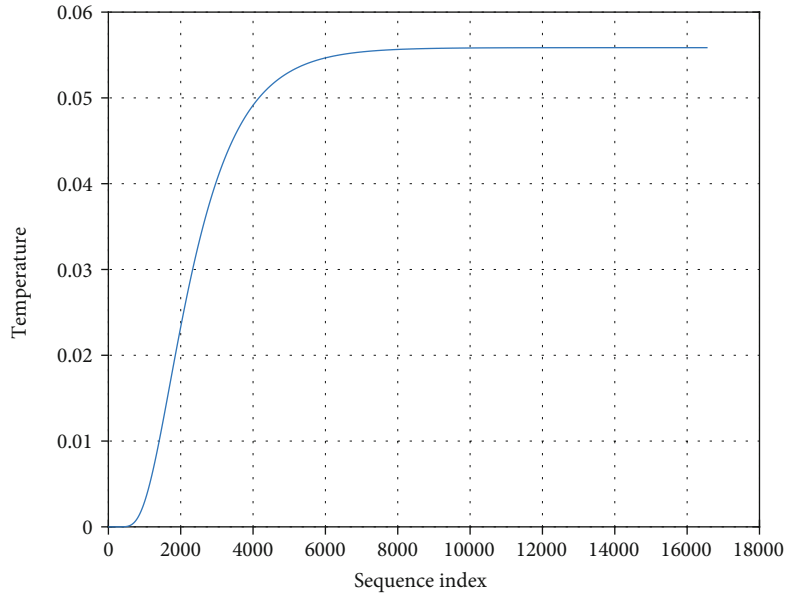

Figure 8: Sequence behavior at point 1.0.

Figure 2 also shows that such increase in the number of iterations is linear to the increase in the value of α; however this linearity is valid in the region where α is large.

For values of α close to zero, it can be noticed that the number of iterations varies, seeking to approach linearity as it moves away from values close to zero, as can be seen in Figure 3.

Disregarding the variation in computational effort for each α due to the increase in the number of iterations, the thermal profile of the fin is identical for any α and is given by Figure 4.

The convergence of the numerical sequence can be noticed, according to the adopted parameters, through the visualization of a well-behaved curve, where after a certain point, there is no longer a considerable difference between previous values.

It is interesting to analyze the behavior of the numerical convergence of specific points on the fin, since, for comparative purposes, the variation in the convergence speed is noted. For this, the points were analyzed: 0.25, 0.5, 0.75, and 1.0, as illustrated in Figures 5–8.

It is possible to better visualize how the parameters of temperature, sequence elements, and fin nodal points vary in a combined way through Figure 9.

Thus, as expected, it is noted that convergence occurs more quickly at points closer to the base.

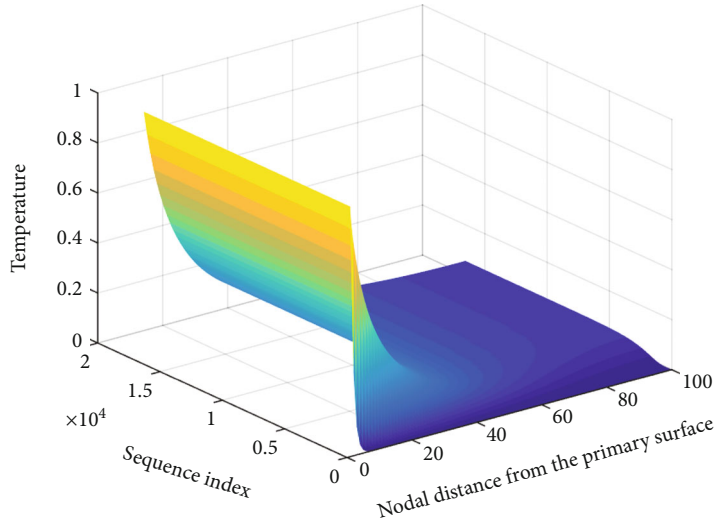

Figure 9: Result surface.

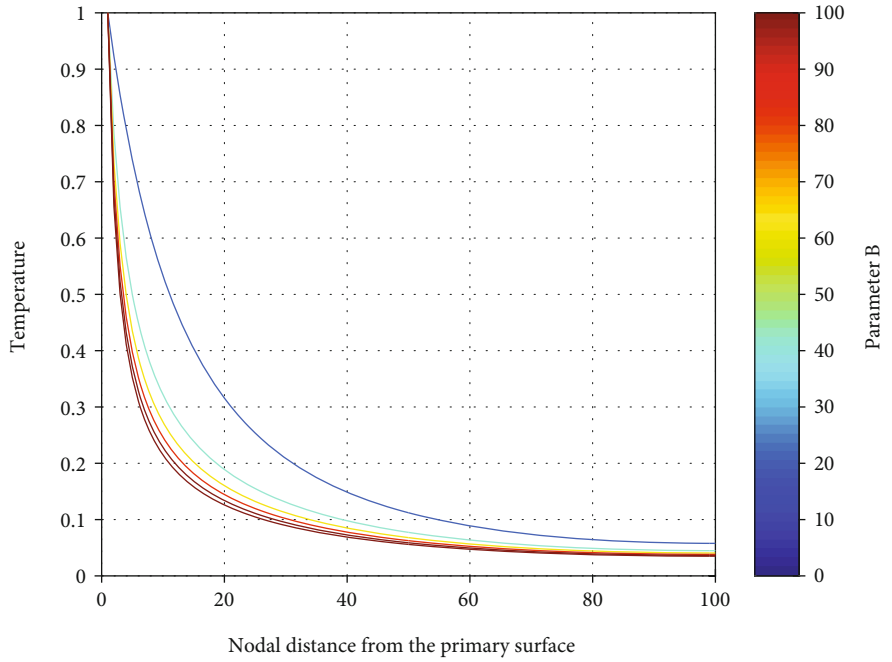

Figure 10: Thermal radiation influence analysis.

In order to further analyze the influence of radiation on the thermal profile that was modeled in this work, it was studied how the variation of the parameter B affects the temperature distribution along a porous radial fin. For this, the parameter B was taken with different values, where such values were compared with the situation where $B = 0$. The consideration of $B = 0$ implies a situation where thermal radiation is not considered; that is, the nonlinear temperature term due to radiation is removed from the modeling. It is noteworthy that disregarding the effects of thermal radiation greatly alters the problem analyzed, since the radiation emitted by the fin through its pores considerably affects how the temperature is dissipated in the body.

Figure 10 shows six superimposed temperature profiles, in which the value of the parameter B varies from $B = 0$ (a situation that disregards the effects of thermal radiation), increasing the value of B, passing by $B = 20$, $B = 40$, $B = 60$, $B = 80$, up to $B = 100$.

For a better analysis, Table 1 shows the dimensionless values of the temperature in some selected nodes, comparing such values for the situations where $B = 0$ with $B = 20$.

Table 1: Comparison of radiation values $B = 20$.

Node	$B = 0$	$B = 20$	$B_{20} - B_0$	%
1	1.0000	1.0000	0.0000	0.00%
2	0.9228	0.7862	0.1366	14.80%
5	0.7381	0.4996	0.2385	32.31%
10	0.5334	0.3219	0.2115	39.65%
20	0.3157	0.1889	0.1268	40.16%
30	0.2087	0.1308	0.0779	37.33%
40	0.1486	0.0979	0.0507	34.12%
50	0.1121	0.0773	0.0348	31.07%
60	0.0888	0.0637	0.0252	28.32%
70	0.0738	0.0546	0.0191	25.94%
80	0.0644	0.0489	0.0155	24.07%
90	0.0593	0.0457	0.0136	22.88%
100	0.0578	0.0448	0.0130	22.49%

Table 2: Comparison of radiation values $B = 40$.

Node	$B = 0$	$B = 40$	$B_{40} - B_0$	%
1	1.0000	1.0000	0.0000	0.00%
2	0.9228	0.7343	0.1885	20.43%
5	0.7381	0.4348	0.3033	41.09%
10	0.5334	0.2731	0.2603	48.80%
20	0.3157	0.1603	0.1555	49.24%
30	0.2087	0.1122	0.0965	46.24%
40	0.1486	0.0851	0.0636	42.76%
50	0.1121	0.0680	0.0441	39.38%
60	0.0888	0.0566	0.0322	36.27%
70	0.0738	0.0490	0.0247	33.54%
80	0.0644	0.0442	0.0202	31.38%
90	0.0593	0.0415	0.0178	29.99%
100	0.0578	0.0407	0.0171	29.54%

Table 3: Comparison of radiation values $B = 60$.

Node	$B = 0$	$B = 60$	$B_{60} - B_0$	%
1	1.0000	1.0000	0.0000	0.00%
2	0.9228	0.7006	0.2222	24.08%
5	0.7381	0.3975	0.3406	46.15%
10	0.5334	0.2462	0.2873	53.85%
20	0.3157	0.1445	0.1713	54.24%
30	0.2087	0.1018	0.1069	51.22%
40	0.1486	0.0778	0.0709	47.69%
50	0.1121	0.0625	0.0496	44.21%
60	0.0888	0.0524	0.0364	40.97%
70	0.0738	0.0457	0.0281	38.11%
80	0.0644	0.0413	0.0231	35.84%
90	0.0593	0.0389	0.0204	34.36%
100	0.0578	0.0382	0.0196	33.89%

Table 4: Comparison of radiation values $B = 80$.

Node	$B = 0$	$B = 80$	$B_{80} - B_0$	%
1	1.0000	1.0000	0.0000	0.00%
2	0.9228	0.6756	0.2472	26.79%
5	0.7381	0.3717	0.3664	49.64%
10	0.5334	0.2281	0.3054	57.24%
20	0.3157	0.1339	0.1819	57.60%
30	0.2087	0.0947	0.1140	54.61%
40	0.1486	0.0727	0.0759	51.08%
50	0.1121	0.0588	0.0533	47.57%
60	0.0888	0.0495	0.0393	44.28%
70	0.0738	0.0433	0.0305	41.36%
80	0.0644	0.0393	0.0251	39.03%
90	0.0593	0.0371	0.0222	37.51%
100	0.0578	0.0364	0.0214	37.02%

Table 5: Comparison of radiation values $B = 100$.

Node	$B = 0$	$B = 100$	$B_{100} - B_0$	%
1	1.0000	1.0000	0.0000	0.00%
2	0.9228	0.6557	0.2671	28.95%
5	0.7381	0.3523	0.3858	52.27%
10	0.5334	0.2146	0.3188	59.76%
20	0.3157	0.1260	0.1897	60.09%
30	0.2087	0.0895	0.1192	57.14%
40	0.1486	0.0689	0.0797	53.63%
50	0.1121	0.0559	0.0562	50.12%
60	0.0888	0.0472	0.0416	46.81%
70	0.0738	0.0414	0.0324	43.87%
80	0.0644	0.0377	0.0267	41.50%
90	0.0593	0.0356	0.0237	39.97%
100	0.0578	0.0350	0.0228	39.47%

Increasing the value of B means increasing the influence of the effects of thermal radiation. It is interesting to take this increment gradually, so that it is possible to analyze the thermal behavior of the fin as the radiation becomes considerable. Thus, analyzing the thermal profile for the value of $B = 40$, we have Table 2.

It can be noticed, analyzing Tables 1 and 2, that the greatest discrepancy between temperature values occurs between nodes 10 and 20. As the analysis progresses, the temperature values for $B = 60$ are taken, as seen in Table 3.

Going forward in the analysis of the influence of thermal radiation, it can already be noted that, from here on, large increments in the value of B change the profile little, as can be seen in Table 4.

The analysis ends with the temperature values for $B = 100$ as shown in Table 5, where it is noticed that the thermal profile varies little in relation to values of B a little smaller. The greatest discrepancy between temperature values for $B = 100$ and $B = 80$ is less than 6%, bringing the hypothesis of negligible variation in values much larger in B.

It can be seen, through this analysis, that the parameter that carries the effect of thermal radiation has a great influence on the thermal profile, since the discrepancy in temperature values between profiles with higher values of B reaches more than 60% (comparison between the cases $B = 0$ and $B = 100$).

4. Conclusions

This work provides a comprehensive approach to heat dissipation in extended surfaces, where several parameters were considered, among which the application of thermal radiation effects and the porosity of the fin material stand out. The developed model seeks an adequate solution to the problem, applying a cylindrical geometry, widely used in engineering, mainly in heat dissipation in industrial pipes.

The mathematical description of the solution proves that the model used in this work has an exact solution, which was presented, provided that a specific criterion of nondecrease of the thermal profile is met, which was also mathematically proven.

The simple methodology employed considers realistic modeling of heat transfer with specific boundary conditions in different porous media. Applications of this procedure seeks to extrapolate finned array analysis of heat sinks and the relevance of your parameters on final heat flux.

Appendix

The convexity and coercivity of the functional

$$I[\omega] = \frac{1}{2}\int_1^{\xi_E}\left(\frac{d\omega}{d\xi}\right)^2 \xi d\xi + \frac{A}{3}\int_1^{\xi_E}|\omega - \theta_\infty|^3 \xi d\xi + \frac{B}{5}\int_1^{\xi_E}\left\{|\omega|^5 - 5\omega\theta_\infty^4\right\}\xi d\xi \tag{A.1}$$

guarantee the existence and uniqueness of the solution in minimization. [26]

A.1. Convexity

The convexity demonstration will be divided into 3 functional terms:

(i) $(1/2)\int_1^{\xi_E}(d\omega/d\xi)^2\xi d\xi$

(ii) $(A/3)\int_1^{\xi_E}|\omega - \theta_\infty|^3\xi d\xi$

(iii) $\int_1^{\xi_E}\{|\omega|^5 - 5\omega\theta_\infty^4\}\xi d\xi$

(a) In this term $(1/2)\int_1^{\xi_E}(d\omega/d\xi)^2\xi d\xi$, we take

$$I_1[\omega] = \int_1^{\xi_E}\left(\frac{d\omega}{d\xi}\right)^2 \xi d\xi \tag{A.2}$$

We need to demonstrate that $I_1[t\omega_1 + (1-t)\omega_2] \le tI_1[\omega_1] + (1-t)I_1[\omega_2]$ with $t \in (0;1)$ and $\omega_1 \neq \omega_2$ in the space of admissible functions.

Applying the condition to the functional, we have

$$\begin{aligned}
&\int_1^{\xi_E}\left(\frac{d(t\omega_1 + (1-t)\omega_2)}{d\xi}\right)^2 \xi d\xi \\
&\quad \le t\int_1^{\xi_E}\left(\frac{d\omega_1}{d\xi}\right)^2 \xi d\xi + +(1-t)\int_1^{\xi_E}\left(\frac{d\omega_2}{d\xi}\right)^2 \xi d\xi \\
&\quad \Rightarrow t + (1-t)\int_1^{\xi_E}\left(\frac{d\omega_2}{d\xi}\right)^2 \xi d\xi \\
&\qquad - t^2\int_1^{\xi_E}\left(\frac{d\omega_1}{d\xi}\right)^2 \xi d\xi - -2t(t-1)\int_1^{\xi_E}\frac{d\omega_1}{d\xi} \\
&\qquad \cdot \frac{d\omega_2}{d\xi}\xi d\xi - -(1-t)^2\int_1^{\xi_E}\left(\frac{d\omega_2}{d\xi}\right)^2 \xi d\xi \\
&\quad \ge 0 \Rightarrow \left(t - t^2\right)\int_1^{\xi_E}\left(\frac{d\omega_1}{d\xi}\right)^2 \xi d\xi \\
&\qquad + \left[(1-t) - (1-t)^2\right]\cdots\cdots\int_1^{\xi_E}\left(\frac{d\omega_2}{d\xi}\right)^2 \xi d\xi \\
&\qquad + 2\left(t - t^2\right)\int_1^{\xi_E}\frac{d\omega_1}{d\xi}\cdot\frac{d\omega_2}{d\xi}\xi d\xi \ge 0.
\end{aligned} \tag{A.3}$$

For $t \in (0;1)$, we have $t - t^2 > 0$. Thus, the function $I_1[\omega]$ is nonnegative.

(b) The term $(A/3)\int_1^{\xi_E}|\omega - \theta_\infty|^3\xi d\xi$ has the 2 variation $(A/3)\int_1^{\xi_E}6|\omega - \theta_\infty|\xi d\xi$ which is strictly positive with ω different from constant

(c) The term $(B/5)\int_1^{\xi_E}\{|\omega|^5 - 5\omega\theta_\infty^4\}\xi d\xi$ has the 2 variations of the 1 parcel equal to $(B/5)\int_1^{\xi_E}|20\omega|^3\xi d\xi$ which is strictly positive with ω different from constant. The 2 portions are a linear term that does not influence the convexity of the functional

Thus, the functional $I[\omega]$ is convex.

A.2. Coerciveness

The functional 27 is coercive if

$$\lim_{\gamma\longrightarrow+\infty}\left(\frac{I[\gamma\omega]}{\gamma}\right) = +\infty. \tag{A.4}$$

For the purpose of coerciveness, we will take $\|\omega\| = 1$, with $\omega \in H$.

We have

$$I[\gamma\omega] = \frac{1}{2}\int_1^{\xi_E}\left(\frac{d\gamma\omega}{d\xi}\right)^2\xi d\xi + \frac{A}{3}\int_1^{\xi_E}|\gamma\omega-\theta_\infty|^3\xi d\xi + \frac{B}{5}\int_1^{\xi_E}\left(|\gamma\omega|^5-5\gamma\omega\theta_\infty^4\right)\xi d\xi \Rightarrow I[\gamma\omega] = \frac{\gamma^2}{2}\int_1^{\xi_E}\left(\frac{d\omega}{d\xi}\right)^2\xi d\xi + \frac{A}{3}|\gamma|^3\int_1^{\xi_E}\left|\omega-\frac{\theta_\infty}{\gamma}\right|^3\xi d\xi + \frac{B}{5}|\gamma|^5\int_1^{\xi_E}\left(|\omega|^5-\frac{\omega\theta_\infty^4}{|\gamma|^4}\right)\xi d\xi. \tag{A.5}$$

So,

$$\frac{I[\gamma\omega]}{\gamma} = \frac{\gamma}{2}\int_1^{\xi_E}\left(\frac{d\omega}{d\xi}\right)^2\xi d\xi + \frac{A}{3}|\gamma|^2\int_1^{\xi_E}\left|\omega-\frac{\theta_\infty}{\gamma}\right|^3\xi d\xi + \frac{B}{5}|\gamma|^4\int_1^{\xi_E}\left(|\omega|^5-\frac{\omega\theta_\infty^4}{|\gamma|^4}\right)\xi d\xi, \tag{A.6}$$

in which

$$\lim_{\gamma\longrightarrow+\infty}\left(\frac{A}{3}|\gamma|^2\int_1^{\xi_E}\left|\omega-\frac{\theta_\infty}{\gamma}\right|^3\xi d\xi\right) = \begin{cases}+\infty, & \text{if } \omega\neq\text{constant},\\ +\infty, & \text{if } \omega=\text{constant},\end{cases}$$

$$\lim_{\gamma\longrightarrow+\infty}\left(\frac{\gamma}{2}\int_1^{\xi_E}\left(\frac{d\omega}{d\xi}\right)^2\xi d\xi\right) = \begin{cases}+\infty, & \text{if } \omega\neq\text{constant},\\ 0, & \text{if } \omega=\text{constant},\end{cases}$$

$$\lim_{\gamma\longrightarrow+\infty}\left(\frac{B}{5}|\gamma|^4\int_1^{\xi_E}\left(|\omega|^5-\frac{\omega\theta_\infty^4}{|\gamma|^4}\right)\xi d\xi\right) = \begin{cases}+\infty, & \text{if } \omega\neq\text{constant},\\ 0, & \text{if } \omega=\text{constant}.\end{cases} \tag{A.7}$$

Hence, the equality 30 is true.

Symbols

A: Porous parameter
A_c: Cross-sectional area
B: Radiation parameter
c_p: Specif heat
$\vec{g}$: Gravitational acceleration
h: Convective coefficient
k: Thermal conductivity
k_{eff}: Effective thermal conductivity of porous media
K: Permeability of the porous fin
$\dot{m}$: Mass flow rate
P: Fin perimeter
q: Heat transfer rate
r: Radial coodinate
R: Fin radius
t: Fin thickness
T: Temperature
v_w: Fluid velocity
W: Width of the fin
x: Axial coordinate

Greek Symbols

α_f: Thermal diffusivity
β_f: Thermal expansion coefficient
Δ: Temperature difference
ε: Emissivity
φ: Solution sequence elements
σ: StephenBoltzmann constant
ν: Kinematic viscosity
ρ: Fluid density.

Data Availability

The data used to support the findings of this study are available within the article.

Conflicts of Interest

The authors declare that there are no conflicts of interest regarding the publication of this paper.

Acknowledgments

The author R. M. S. Gama gratefully acknowledges the support provided by Brazilian Agency CNPq (Grant 306364/2018-1). In addition, all the authors acknowledge the support provided by the Coordenação de Aperfeiçoamento de Pessoal de Nvel Superior Brasil (CAPES Finance Code 001).

References

[1] M. Mhlongo and R. Moitsheki, "Some exact solutions of nonlinear fin problem for steady heat transfer in longitudinal fin with different profiles," *Advances in Mathematical Physics*, vol. 2014, 16 pages, 2014.

[2] A.-R. Khaled, "Mathematical extrapolating of highly efficient fin systems," *Mathematical Problems in Engineering*, vol. 2011, 18 pages, 2011.

[3] C. Harley, "Asymptotic and dynamical analyses of heat transfer through a rectangular longitudinal fin," *Journal of Applied Mathematics*, vol. 2013, 8 pages, 2013.

[4] A. Arulselvan, V. Pandiyarajan, and R. Velraj, "Experimental investigation of the thermal performance of a heat pipe under various modes of condenser cooling," *Heat Transfer Research*, vol. 48, no. 13, pp. 1151–1164, 2017.

[5] M. H. Elnaggar, M. Abdullah, and M. A. Mujeebu, "Experimental analysis and fem simulation of finned u-shape multi heat pipe for desktop pc cooling," *Energy Conversion and Management*, vol. 52, no. 8-9, pp. 2937–2944, 2011.

[6] G. Righetti, C. Zilio, S. Mancin, and G. A. Longo, "Heat pipe finned heat exchanger for heat recovery: experimental results and modeling," *Heat Transfer Engineering*, vol. 39, no. 12, pp. 1011–1023, 2018.

[7] F. Mabood, W. A. Khan, and A. I. Md Ismail, "Series solution for steady heat transfer in a heat-generating fin with convection and radiation," *Mathematical Problems in Engineering*, vol. 2013, 7 pages, 2013.

[8] J. M. Quirino, E. D. Correa, R. L. Sobral, and R. M. S. da Gama, "The Kirchhoff transformation for convective-radiative thermal problemsin fins," *International Journal of Mechanics*, vol. 15, pp. 12–21, 2021.

[9] I. Pop, J. Sunada, P. Cheng, and W. Minkowycz, "Сопряженная своБодная конвекция при Больших числач релея от длинных вертикаляных плоских реБер, погруженных в пористую среду," *International Journal of Heat and Mass Transfer*, vol. 28, no. 9, pp. 1629–1636, 1985.

[10] P. Huang and K. Vafai, "Analysis of forced convection enhancement in a channel using porous blocks," *Journal of Thermophysics and Heat Transfer*, vol. 8, no. 3, pp. 563–573, 1994.

[11] S. Kim, J. Paek, and B. Kang, "Flow and heat transfer correlations for porous fin in a plate-fin heat exchanger," *Journal of Heat Transfer*, vol. 122, no. 3, pp. 572–578, 2000.

[12] S. Kiwan, "Thermal analysis of natural convection porous fins," *Transport in Porous Media*, vol. 67, no. 1, pp. 17–29, 2007.

[13] M. El-Hakiem and A. M. Rashad, "Effect of radiation on non-darcy free convection from a vertical cylinder embedded in a fluidsaturated porous medium with a temperature-dependent viscosity," *Journal of Porous Media*, vol. 10, no. 2, pp. 209–218, 2007.

[14] A. Rashad, "Influence of radiation on MHD free convection from a vertical flat plate embedded in porous media with thermophoretic deposition of particles," *Communications in Nonlinear Science and Numerical Simulation*, vol. 13, no. 10, pp. 2213–2222, 2008.

[15] B. Kundu and D. Bhanja, "Prevision, analytique de la performance et la conception optimale d'ailettes poreuses," *International Journal of Refrigeration*, vol. 34, no. 1, pp. 337–352, 2011.

[16] R. S. R. Gorla and A. Bakier, "Thermal analysis of natural convection and radiation in porous fins," *International Communications in Heat and Mass Transfer*, vol. 38, no. 5, pp. 638–645, 2011.

[17] S. El-Kabeir, A. J. Chamkha, and A. M. Rashad, "Effect of thermal radiation on non-darcy natural convection from a vertical cylinder embedded in a nanofluid porous media," *Journal of Porous Media*, vol. 17, no. 3, pp. 269–278, 2014.

[18] A. Rashad, B. Mallikarjuna, A. Chamkha, and S. H. Raju, "Thermophoresis effect on heat and mass transfer from a rotating cone in a porous medium with thermal radiation," *Afrika Matematika*, vol. 27, no. 7-8, pp. 1409–1424, 2016.

[19] M. Darvishi, R. Gorla, and F. Khani, "Natural convection and radiation in porous fins," *International Journal of Numerical Methods for Heat & Fluid Flow*, vol. 23, no. 8, pp. 1406–1420, 2013.

[20] M. Darvishi, R. S. R. Gorla, and F. Khani, "Unsteady thermal response of a porous fin under the influence of natural convection and radiation," *Heat and Mass Transfer*, vol. 50, no. 9, pp. 1311–1317, 2014.

[21] M. Darvishi, R. S. R. Gorla, F. Khani, and B. Gireesha, "Thermal analysis of natural convection and radiation in a fully wet porous fin," *International Journal of Numerical Methods for Heat & Fluid Flow*, vol. 26, no. 8, pp. 2419–2431, 2016.

[22] G. Sobamowo, "Analysis of heat transfer in porous fin with temperature-dependent thermal conductivity and internal heat generation using chebychev spectral collocation method," *Journal of Computational Applied Mechanics*, vol. 48, no. 2, pp. 271–284, 2017.

[23] R. Jooma and C. Harley, "Heat transfer in a porous radial fin: analysis analysis of numerically obtained solutions," *Advances in Mathematical Physics*, vol. 2017, 20 pages, 2017.

[24] G. Sowmya, B. Gireesha, and H. Berrehal, "An unsteady thermal investigation of a wetted longitudinal porous fin of different profiles," *Journal of Thermal Analysis and Calorimetry*, vol. 143, no. 3, pp. 2463–2474, 2021.

[25] R. M. S. da Gama, "Existence uniqueness and construction of the solution of the energy transfer problem in a rigid and non-convex black body," *Zeitschrift f¨ur angewandte Mathematik und Physik ZAMP*, vol. 42, no. 3, pp. 334–347, 1991.

[26] M. Berger, *Nonlinearity and Functional Analysis*, Academic Press, 1977.